INTERNATIONAL JOURNAL OF FLUID POWER
2018, VOL. 19, NO. 2, 106–116
https://doi.org/10.1080/14399776.2018.1476306

Taylor & Francis
Taylor & Francis Group

ARTICLE

Understanding overall efficiency of hydrostatic pumps and motors

Gustavo Koury Costa[a] and Nariman Sepehri[b]

[a]Department of Mechanics, Federal Institute of Science and Technology of the State of Pernambuco, Recife, Brazil; [b]Department of Mechanical Engineering, University of Manitoba, Winnipeg, MB, Canada

ABSTRACT

Pump and motor efficiency is a complex subject, to such an extent that most of the available models describing efficiency today rely on experimental data. In spite of that, mathematical models relating efficiency to pressure and angular speed have been proposed throughout the years. In all these models, volumetric and mechanical efficiencies are separately built from flow and torque losses relations. The overall efficiency model is then obtained by multiplying the volumetric and the mechanical efficiency equations. In this paper, we show that the overall efficiency equations must be developed from an energy balance and show that the simple multiplication of mechanical and volumetric efficiencies can potentially lead to inaccurate results. We then obtain a generalised equation relating the overall efficiency to pressure and angular speed for both pumps and motors and show how the resulting model can be fitted to actual experimental data.

ARTICLE HISTORY
Received 2 December 2017
Accepted 11 May 2018

KEYWORDS
Hydraulic pumps; hydraulic motors; overall efficiency

1. Introduction

Many attempts have been made to build an analytical model that could describe as accurately as possible the volumetric and torque losses in hydrostatic pumps and motors (see Jung *et al.* 2005). In fact, modelling losses using experimental data instead of efficiency has been reported to be the preferred way to proceed (KohmäScher *et al.* 2007). In what concerns to overall efficiency modelling, the typical procedure is to first write the volumetric and mechanical efficiencies in terms of the volumetric and torque losses, and multiply the expressions for those efficiencies to obtain the overall efficiency equation. This definition of overall efficiency as being the product of mechanical and volumetric efficiencies has long been assumed as correct (see Wilson 1949, Manring 2005a). In this paper, we show that multiplying mechanical and volumetric efficiencies will not necessarily result in a correct overall efficiency model. Moreover, we demonstrate that even simple loss models can approximate overall efficiency curves when the right definition of efficiency is used.

2. Literature review and problem description

2.1. *Leakage and friction losses*

It was back in 1946 when W.E. Wilson published his pioneering paper on rotary pump and motor efficiencies (Wilson 1946). In his theory, leakage flows within pumps and motors were seen as the sum of laminar viscous flows between infinite parallel plates. Turbulent loss equations were also suggested without a formal proof. Wilson based his analysis on an external gear unit, as shown in Figure 1(a), and focused on the gear-case gaps, where leakages are likely to take place. Further, he assumed that the pump/motor leakages could be thought as the flow between a moving and a stationary surface subject to a pressure differential, $p = p_1 - p_2$, as shown in Figure 1(b). Under certain assumptions, it can be shown that the fluid speed within the gear-case gap in the laminar regime, $u(y)$, is given by:

$$u(y) = \left(\frac{R\omega}{C}\right)y - \frac{p}{2\mu L}\left(y^2 - Cy\right) \tag{1}$$

where μ is the absolute viscosity. The other terms in Equation (1) are represented in Figure 1. Note that we can associate the first term in Equation (1) with a Couette flow, caused by the dragging of fluid by the moving plate when $p = 0$. Similarly, the second term can be associated to a Poiseuille flow, caused by the pressure differential, p, when both plates are stationary ($\omega = 0$).

Remark. The pressure within the teeth spaces changes continuously from p_1 to p_2, along the fluid path between the input and output ports. Therefore, Figure 1(b) cannot represent a tooth-case gap, as indicated in the figure, because the pressures at both extremities of the tooth are not known. However, we may think of Figure 1(b) as representing the summation of all tooth-case gaps between the input and output ports, which justifies the use of the limiting pressures, p_1 and p_2, as indicated.

CONTACT Nariman Sepehri Nariman.Sepehri@umanitoba.ca Department of Mechanical Engineering, University of Manitoba, Winnipeg, MB, Canada

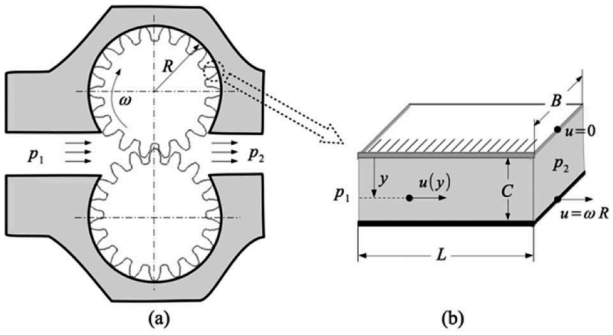

Figure 1. Leaking flow in a gear pump/motor.

To obtain the leaking flow, q_L, for the unit shown in Figure 1, Wilson multiplied $u(y)$ by the gear thickness, B, and integrated between $y = 0$ and $y = C$:

$$q_L = \left(\frac{RBC}{2}\right)\omega + \left(\frac{BC^3}{12\mu L}\right)p \tag{2}$$

The torque loss, T_L, was obtained by considering the viscous forces acting on the moving surface, at $y = C$:

$$T_L = \left[BL\left(\mu\frac{du}{dy}\right)_{y=C}\right]R = \left(\frac{R^2BL}{C}\right)\mu\omega - \left(\frac{RBC}{2}\right)p \tag{3}$$

From Equations (2) and (3), it is apparent that both volumetric and torque losses depend on the angular speed, ω, and the pressure differential, p. Consider now the motoring operation of the gear unit shown in Figure 1, where $p_1 > p_2$. We can write the following equations for the input flow, q_m, and the shaft torque, T_m, based on Equations (2) and (3) and the volumetric displacement, D, expressed in units of volume per radian:
where

$$\begin{cases} q_m = D\omega + q_L = (D + K_u)\omega + K_s\frac{p}{\mu} \\ T_m = pD - T_L = (D + K_u)p - K_\omega\mu\omega \end{cases} \tag{4}$$

$$K_u = \frac{RBC}{2};\ K_s = \frac{BC^3}{12L} \text{ and } K_\omega = \frac{R^2BL}{C} \tag{5}$$

Wilson identified the term $D + K_u$ in Equation (4), as the 'total displacement', D^*, resulting from the sum of the geometrical displacement, D, and the 'gear-case clearance displacement', K_u, where fluid is dragged along, by the action of viscous forces. Note that if we consider the gear unit in Figure 1 operating as a pump, i.e. $p_1 < p_2$, the following equations for the output flow, q_p, and the input torque, T_p, are obtained:

$$\begin{cases} q_p = D\omega - q_L = (D - K_u)\omega - K_s\frac{p}{\mu} \\ T_p = pD + T_L = (D - K_u)p + K_\omega\mu\omega \end{cases} \tag{6}$$

Note that in Equation (6), the total displacement D^* should be redefined as $D^* = D - K_u$. Reethof (Blackburn *et al.* 1960), followed another approach, in which he disregarded the term K_u for being 'very small' because of the small gear-housing clearance, C. Although the idea seems to have prevailed in most of the models proposed till recently (see for instance Jung *et al.* 2005), we believe that the assumption that K_u can be disregarded must be revisited. In fact, from Equation (5), we see that the relative value of K_u with respect to the other coefficients, K_s and K_ω, is given by

$$\begin{cases} \frac{K_u}{K_s} = \frac{12LRBC}{2BC^3} = \frac{6LR}{C^2} \\ \frac{K_u}{K_\omega} = \frac{RBC^2}{2R^2BL} = \frac{C^2}{2RB} \end{cases} \tag{7}$$

In a typical gear pump, the gear-case clearance, C, is of order 10^{-5}m (Doddannavar and Barnard 2005); while R and B are of order 10^{-2}m. On the other hand, the gear teeth thickness, L, is typically of order 10^{-3}m. Thus, from Equation (7), we observe that K_u is very small with respect to K_ω, but not with respect to K_s, which means that K_u should not be disregarded in the volumetric loss Equations (4) and (6). With these considerations, we may rewrite Equations (4) and (6) as:

$$\begin{cases} q_p = D\omega - K_u\omega - K_s\frac{p}{\mu} \\ T_p = Dp + K_\omega\mu\omega \\ q_m = D\omega + K_u\omega + K_s\frac{p}{\mu} \\ T_m = Dp - K_\omega\mu\omega \end{cases} \tag{8}$$

Interestingly, the term $K_u\omega$ is not present in many volumetric loss models (Jung *et al.* 2005). However, Dorey (1988) quoted the work of Tessmann (1979), in which a term proportional to the angular speed appeared in the volumetric loss equations. Dorey also quoted the work of Zarotti and Nervegna (1981) on axial pump/motor units in which a nonlinear term where the volumetric losses appear as a function of $\omega^{1.5}$ was included. In any case, these additions apparently came out of experimental observation rather than theory. One exception can be found in the recent work done by Jeong (2007), where a theoretical model for axial piston motors was developed.

Although the presence of a term proportional to the angular speed, ω, in the volumetric loss equation

is not widely accepted, most researches have included a term proportional to the pressure differential, $K_p p$, in their torque loss equations. Such term, though mathematically identical to $K_u p$, which we disregarded when moving from Equations (4) and (6) to Equation (8), carries a totally different meaning and, again, has been justified by experiment rather than theory. Here, the coefficient K_p is related to the dry friction (Coulomb friction) between the moving parts of the machine. The association of the term $K_p p$ with the Coulomb friction was also pointed out by Wilson (1946), though it was never formally proved. Dorey (1988) offered a simple explanation where he assumed that the dry friction torque, T_f, could be written as a fraction of the ideal torque, Dp, i.e. $T_f = C_f(Dp) = K_p p$, where C_f is the Coulomb friction coefficient. Reethof (Blackburn *et al.* 1960), justified the use of $K_p p$ based on experimental observations.

The following pump loss equations were introduced by Wilson (1949), which are a modified version of Equation (8) where K_u is considered zero and other terms are added to better fit the experimental results:

$$\begin{cases} q_p = D\omega - C_s D\frac{p}{\mu} - q_r \\ T_p = Dp + C_\omega D\mu\omega + C_p Dp + T_c \end{cases} \tag{9}$$

Although the coefficients K_s, K_ω and K_p are not explicitly show in Equation (9), similar coefficients can be easily obtained by a simple association of terms. The coefficients C_s, C_ω and C_p must be experimentally determined and the new terms q_r and T_c account for 'cavitation losses' and 'pressure-independent friction losses', respectively. Interestingly, the terms q_r and T_c are not present in other models, as summarised by Jung *et al.* (2005). In fact, as will be shown later in this paper, the exact meaning of these terms is not well defined as they may become negative when experimental data are fitted into the mathematical model (9). We thus see q_r and T_c as having a corrective role to compensate for errors in the determination of the pump and motor flow and torques, due to imprecisions in pressure, displacement and speed measurements (Manring 2005b). We then have chosen to change the notation introduced by Wilson and use q_0 and T_0 instead of q_r and T_c hereafter.

Note the presence of the displacement, D, multiplying the loss terms in Equation (9). This was not present in Wilson's first paper and cannot be easily justified from Equation (6). However, it has been assumed as correct and naturally included in subsequent works, such as McCandlish and Dorey (1984), Dorey (1988) and Jung *et al.* (2005). Observe that for fixed-displacement units, D is constant and the terms $C_s D$, $C_\omega D$ and $C_p D$ become mathematically identical to K_s, K_ω and K_p. This is the rationale followed by McCandlish and Dorey (1984) who proposed the following equations for variable-displacement pumps, in the absence of compressibility losses:

$$\begin{cases} q_p = xD_m\omega - C_s D_m\frac{p}{\mu} \\ T_p = xD_m p + C_\omega D_m\mu\omega + C_p D_m p \end{cases} \tag{10}$$

In Equation (10), D_m is the maximum displacement of the pump and xD_m is the actual pump displacement ($0 \le x \le 1$). Observe that the loss terms $C_s D_m$, $C_\omega D_m$ and $C_p D_m$ are not affected by the actual displacement. Therefore, we can consider $C_s D_m = K_s$, $C_\omega D_m = K_\omega$ and $C_p D_m = K_p$ and write the following modified version of Wilson's model for variable-displacement units:

$$\begin{cases} q_p = xD_m\omega - K_s\frac{p}{\mu} - q_0 \\ T_p = xD_m p + K_\omega\mu\omega + K_p p + T_0 \\ q_m = xD_m\omega + K_s\frac{p}{\mu} + q_0 \\ T_m = xD_m p - K_\omega\mu\omega - K_p p - T_0 \end{cases} \tag{11}$$

Remarks

(1) In Equation (11), only the coefficients K_s and K_ω can be traced back to the gear-case gap analysis carried out with the help of Figure 1. The Couette flow term, K_u, does not appear in the volumetric loss equations, though it should not be numerically insignificant in this case (see comments on Equation (7));

(2) The term K_p has been assumed to be proportional to the Coulomb friction between the moving parts. This term has been pointed out as being responsible for the metal-to-metal wearing of the pump/motor parts (Blackburn *et al.* 1960);

(3) Although the theory behind Equation (11) has been based on an external gear unit, they have been equally used for every type of hydrostatic pumps and motors. In fact, Wilson, himself, applied these equations to axial-piston pumps in his second paper (Wilson 1949).

(4) For the reasons explained earlier, we advocate the use of the term $K_u\omega$ in the volumetric loss models. Therefore, we propose that the following modified version of Equation (11) provides a more realistic approximation

$$\begin{cases} q_p = xD_m\omega - K_u\omega - K_s\frac{p}{\mu} - q_0 \\ T_p = xD_m p + K_\omega\mu\omega + K_p p + T_0 \\ q_m = xD_m\omega + K_u\omega + K_s\frac{p}{\mu} + q_0 \\ T_m = xD_m p - K_\omega\mu\omega - K_p p - T_0 \end{cases} \tag{12}$$

2.2. *Fluid compressibility*

Some authors have considered the flow lost through the compressibility of the fluid, q_β ('compressibility flowrate', according to Stringer 1976) in their loss equations:

$$q_\beta = \left(\frac{p}{\beta}\right) D\omega \tag{13}$$

where β is the fluid bulk modulus.

Equation (13) describes the output flow reduction in a pump operating at steady-state regime and has been adopted by the ISO 4391–1983 Standards.

The use of the term 'compressibility losses' has been discussed. For instance, it was argued that while the volumetric flow is decreased, the mass flow remains the same because of the proportional density increment (Ivantysyn and Ivantysynova 2000). Also, for typical pressure values, the quotient p/β in Equation (13) is relatively small. Therefore, as has been done in other models (e.g. Kluger *et al.*, 1996), we have considered $q_\beta = 0$ in our equations.

2.3. Model adjustments

In order to adjust Wilson's model to different situations, empirical terms have been added to Equation (11). The idea has always been to adjust the loss models to experimental data. The resulting models, therefore, lack the physical meaning of the additional terms. A representative list of available loss models can be found in Jung *et al.* (2005) and Hall and Steward (2014). In an attempt to create an unified model to represent any hydrostatic pump or motor, McCandlish and Dorey (1984) proposed a physical-mathematical approach in which the constants in Wilson's model were substituted by products of conveniently chosen functions, whose unknown terms could be obtained through data interpolation. For example, instead of using the constant term, K_s, in Equation (11), the following approximation was proposed (Dorey 1988):

$$K_s = A_s f(p) g(\omega) \tag{14}$$

where A_s is constant; f and g are arbitrary functions of p and ω, usually polynomials.

Strictly speaking, attempting to generalise Wilson's model to fit every type of pump and motor proposed by McCandlish and Dorey has an important drawback. It, actually, leads to a mathematical model that is nonphysical. For example, suppose that we use $K_s = a + b\omega + c\omega^2$ in the volumetric loss equation for the pump, in Equation (11), where the constants a and b, must be experimentally determined. The resulting model becomes:

$$q_p = xD_m\omega - a\frac{p}{\mu} - b\frac{\omega p}{\mu} - c\frac{\omega^2 p}{\mu} - q_0 \tag{15}$$

Although Equation (15) may better suit the experimental data, we end up with the term $\omega^2 p$, for which there is no immediate explanation.

It is always possible to resort to pure mathematical interpolation to represent pump and motor losses, in which case, the approach shifts completely from physical to mathematical, as in the model proposed by Ivantysyn and Ivantysynova (2000), which, as reported by Hall and Steward (2014) and has been well recognised in industry.

2.4. Generalised *first degree loss model*

According to Hall and Steward (2014), loss models can be divided into three categories: Physical, Analytical and Numerical. Physical loss models are those for which a physical explanation can be found for every term in the mathematical model, such as those introduced in Sections 1.1 and 1.2. Analytical loss models make use of interpolation functions to better approximate the coefficients obtained from a physical approach, as discussed in Section 1.3. Numerical loss models are purely built upon data interpolation using suitable mathematical expressions without necessarily having a physical meaning.

Note that all physical loss models presented in Section 1.1 can be conveniently written as:

$$\begin{cases} q_L = \phi_1\omega + k_s p + \phi_3 q_0 \\ T_L = k_\omega\omega + \phi_2 p + \phi_3 T_0 \end{cases} \tag{16}$$

where $k_\omega = K_\omega\mu$ and $k_s = K_s/\mu$. The coefficients ϕ_1, ϕ_2 and ϕ_3, on the other hand, depend on the model being used. For instance, if Equation (11) is used, we have $\phi_1 = 0$, $\phi_2 = K_p$ and $\phi_3 = 1$; if Equation (12) is considered, we have that $\phi_1 = K_u$, $\phi_2 = K_p$ and $\phi_3 = 1$.

2.5. Pump and motor efficiency

Pump and motor manufacturers usually provide efficiency charts, which consist of a set of curves relating volumetric and overall efficiency to pressure and angular speed. Mechanical efficiency curves are hardly ever supplied. The volumetric and mechanical efficiencies for pumps and motors, hereby denoted by η_p^v, η_p^m (pump) and η_m^v and η_m^m (motor), are defined as (Blackburn *et al.* 1960, Akers *et al.* 2006, Costa and Sepehri 2015)

$$\begin{cases} \eta_p^v = \frac{D\omega - q_L}{D\omega} \\ \eta_p^m = \frac{Dp}{Dp + T_L} \\ \eta_m^v = \frac{D\omega}{D\omega + q_L} \\ \eta_m^m = \frac{Dp - T_L}{Dp} \end{cases} \tag{17}$$

Typically, the overall efficiency η is written as the product of volumetric and mechanical efficiencies (Blackburn *et al.* 1960, Merritt 1967, Esposito 1980). Thus, using Equations (16) and (17), we obtain the following expressions for the pump and motor overall efficiencies, η_p and η_m

$$\begin{cases} \eta_p = \frac{p(D\omega - q_L)}{\omega(Dp + T_L)} = \frac{(D-\phi_1)\omega p - k_s p^2 - \phi_3 q_0 p}{(D+\phi_2)\omega p + k_\omega \omega^2 + \phi_3 T_0 \omega} \\ \eta_m = \frac{\omega(Dp - T_L)}{p(D\omega + q_L)} = \frac{(D-\phi_2)\omega p - k_\omega \omega^2 - \phi_3 T_0 \omega}{(D+\phi_1)\omega p + k_s p^2 + \phi_3 q_0 p} \end{cases} \tag{18}$$

Equation (18) can be rearranged as follows

$$\begin{cases} a_p\omega^2 + b_p\omega p + c_p p^2 + d_p\omega + e_p p = 0 \\ a_m\omega^2 + b_m\omega p + c_m p^2 + d_m\omega + e_m p = 0 \end{cases} \tag{19}$$

where

$$\begin{cases} a_p = k_\omega \eta_p; \quad a_m = k_\omega \\ b_p = \left(\eta_p - 1\right)D + \phi_1 + \phi_2\eta_p; \\ b_m = \left(\eta_m - 1\right)D + \eta_m\phi_1 + \phi_2 \\ c_p = k_s; \quad c_m = \eta_m k_s \\ d_p = \eta_p\phi_3 T_0; \quad d_m = \phi_3 T_0 \\ e_p = \phi_3 q_0; \quad e_m = \eta_m\phi_3 q_0 \end{cases} \tag{20}$$

Considering the simple case scenario where the coefficients a through e are constants, each equation in (19) represents a rotated conic in the $\omega - p$ plane for every value of the overall efficiency, η_p or η_m. This is certainly true for the models introduced in Section 1.1. Given the most general case where ϕ_1, ϕ_2, k_s and k_ω are functions of ω^k and p^k $(k \geq 0)$, as in the models listed by Jung *et al.* (2005), or when interpolation functions are used, as proposed by McCandlish and Dorey (1984), the curves described by Equations (19) cannot be easily defined.

Figure 2(a) is an illustration of the typical overall efficiency curves provided by pump and motor manufacturers (Watton 2009). Note that the curves can be roughly modelled as rotated conics for a given range of efficiency values. The problem with such approach is that rotated conics are generally given by the following equation, where $f \neq 0$

$$a\omega^2 + b\omega p + cp^2 + d\omega + ep + f = 0 \tag{21}$$

Comparing Equations (19) and (21), we see that for $f = 0$ every constant-efficiency curve must pass through point $(\omega = 0, p = 0)$ when constant values of a through e are used. Consequently, Equations (19) are not able to represent actual overall efficiency curves when simpler volumetric and mechanical efficiency models are employed, as illustrated by Figure 2 (b). This clearly shows the limitation imposed by making $f = 0$ in (21). Therefore, Wilson's model, given by Equations (11), would produce imprecise results. That being said, it is pertinent to wonder whether the overall efficiency model (18) is correct. Indeed, in this paper, we conclude otherwise, as will be explained in the following section.

3. Overall efficiency model based on energy balances

Consider the pump and motor represented in Figure 3. $\mathcal{P}_i$ and $\mathcal{P}_o$ represent the power input and output at the pump and motor shafts, respectively; Q is the mechanical-hydraulic power loss; q_L represents the volumetric flow losses; q_{pi}, q_{po}, q_{mi} and q_{mo} are the input and output flows at the pump and the motor, respectively.

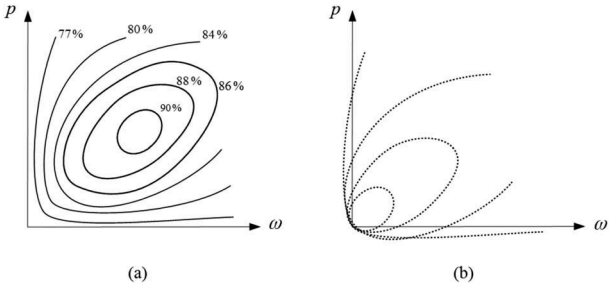

Figure 2. (a) Typical level curves for pump and motor overall efficiencies and (b) curves obtained when $f = 0$.

Assuming that pump and motor are operating at full displacement, we can write for the overall efficiencies, η_p and η_m (Costa and Sepehri 2015. See also Manring 2016, for a similar approach):

$$\begin{cases} \eta_p = \frac{q_{po}p_{po} - q_{pi}p_{pi}}{\mathcal{P}_i} = \frac{q_{po}p_{po} - q_{pi}p_{pi}}{\left(q_{po}p_{po} - q_{pi}p_{pi}\right) + q_L p_{po} + Q} \\ \eta_m = \frac{\mathcal{P}_o}{q_{mi}p_{mi} - q_{mo}p_{mo}} = \frac{(q_{mi}p_{mi} - q_{mo}p_{mo}) - q_L p_{mi} - Q}{q_{mi}p_{mi} - q_{mo}p_{mo}} \end{cases} \tag{22}$$

where p_{pi}, p_{po}, p_{mi} and p_{mo} are the pressures at the pump and motor input and output, respectively. If we make the reasonable assumption that $p_{pi} = p_{mo} = 0$, we can write that $p_{po} = p_{mi} = p$, where p is the pressure differential at the motor/pump ports. As a result, Equation (22) become:

$$\begin{cases} \eta_p = \frac{q_{po}p}{\left(q_{po} + q_L\right)p + Q} \\ \eta_m = \frac{(q_{mi} - q_L)p - Q}{q_{mi}p} \end{cases} \tag{23}$$

We do not know with precision the values of q_{po} and q_{mi} in Equation (23). One possible way to approach the problem is to make $q_{po} = D\omega - q_L$ and $q_{mi} = D\omega + q_L$, in which case we have:

$$\begin{cases} \eta_p = \frac{(D\omega - q_L)p}{D\omega p + Q} \\ \eta_m = \frac{D\omega p - Q}{(D\omega + q_L)p} \end{cases} \tag{24}$$

A crucial step is to correctly define the term Q in Equation (24). We propose the following expression

$$Q = T_L\omega + H_0 \tag{25}$$

where H_0 accounts for any loss that does not vary with speed or pressure. Given that it makes no sense speaking about losses when the pump or motor shaft is not rotating, we implicitly assume that $H_0 = H_0 u(\omega)$, where $u(\omega) = 0$ for $|\omega| = 0$ and $u(\omega) = 1$ for $|\omega| > 0$.

Substituting Q, given by Equation (25), into Equation (24) and using Equation (16) for T_L and q_L, we arrive at the following expressions for η_p and η_m:

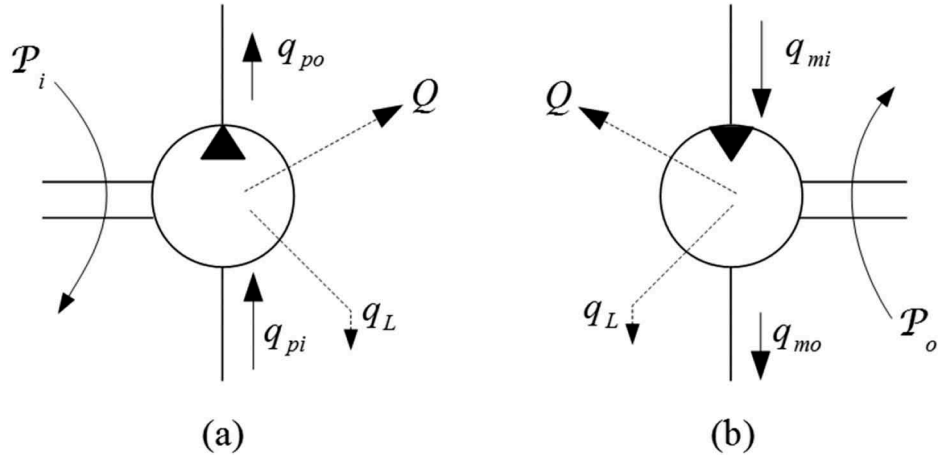

Figure 3. (a) Energy and volumetric flows in a hydrostatic pump and (b) motor.

$$\begin{cases} \eta_p = \frac{(D-\phi_1)\omega p - k_s p^2 - \phi_3 q_0 p}{(D+\phi_2)\omega p + k_\omega \omega^2 + \phi_3 T_0 \omega + H_0} \\ \eta_m = \frac{(D-\phi_2)\omega p - k_\omega \omega^2 - \phi_3 T_0 \omega - H_0}{(D+\phi_1)\omega p + k_s p^2 + \phi_3 q_0 p} \end{cases} \tag{26}$$

Comparing Equation (26) with Equation (18), we see that the denominators of the pump efficiency equations and the numerators of the motor efficiency equations differ by the term H_0. In this sense, multiplying mechanical and volumetric efficiencies overestimates pump efficiency while underestimating motor efficiency.

Remark. Consider the extreme situation where the pump shaft moves very slowly due to an extremely high opposite dry friction torque at the shaft (e.g. caused by a defective roller bearing). In such case, ω will be slightly higher than zero. Consider also that the pressure at the pump output is higher than zero but still relatively low to produce an equally low hydraulic power at the pump output. One would expect the overall efficiency to become very low, given that much energy is being dissipated by friction at the pump shaft ($H_0 \gg 0$) while little hydraulic power is being outputted ($q_{po}p_{po} \to 0$). However, note that the first equation in (18) indicates that $\eta_p \to \infty$ as $\omega \to 0$ for a small output pressure, $p = p_{po} > 0$. Such issue is corrected in Equation (26), where $\eta_p \to 0$ whenever $\omega \to 0$, $p = p_{po} > 0$ and $H_0 \gg 0$. Interestingly, the expressions for η_m in Equations (18) and (26) are qualitatively similar and reasonable even at extreme cases. However, due to the problem with pump efficiency and the difficulty to produce coherent efficiency results when using linear based efficiency models, we favour the use of Equation (26) as the correct efficiency definition.

Each equation in (22) can be developed into the generalised conic Equation (21) with the coefficients $a \ldots f$ given by (subscripts 'p' and 'm' refer to pump and motor, respectively)

$$\begin{cases} a_p = k_\omega \eta_p; \quad a_m = k_\omega \\ b_p = \left(\eta_p - 1\right)D + \phi_1 + \phi_2 \eta_p; \\ b_m = \left(\eta_m - 1\right)D + \eta_m \phi_1 + \phi_2 \\ c_p = k_s; \quad c_m = \eta_m k_s \\ d_p = \eta_p \phi_3 T_0; \quad d_m = \phi_3 T_0 \\ e_p = \phi_3 q_0; \quad e_m = \eta_m \phi_3 q_0 \\ f_p = \eta_p H_0; \quad f_m = H_0 \end{cases} \tag{27}$$

Equations (21) and (27) define a rotated conic curve for each constant value of η_p and η_m. The generated curve, the rotation angle and the displacement in relation to the origin of coordinates, depends on the values of the coefficients a through f. It is important to point out that each coefficient in Equation (21) has a geometrical meaning. The sign of the discriminant $b^2 - 4ac$ defines the type of conic curve we are dealing with

- $b^2 - 4ac > 0$: the curve is a rotated ellipse;
- $b^2 - 4ac = 0$: the curve is a rotated parabola;
- $b^2 - 4ac < 0$: the curve is a rotated hyperbole.

Likewise, the remaining coefficients, d, e and f are also linked to the problem geometry. This can be better understood when we perform a rotation of axis from $\omega - p$ to the rotated system of coordinates $\omega' - p'$, as shown in Figure 4. It can be demonstrated that the general conic Equation (21) in this new coordinate system where $\tan(2\theta) = b/[2(a-c)]$ is

$$\frac{(\omega' + \omega_c)^2}{c} + \frac{(p' + p_c)^2}{a} = r^2 \tag{28}$$

Where

$$\begin{cases} \omega_c = \frac{e}{2a} \\ p_c = \frac{d}{2c} \\ r = \sqrt{\frac{1}{4ac}\left(\frac{e^2}{a} + \frac{d^2}{c} - 4f\right)} \end{cases} \tag{29}$$

With reference to Figure 4, the coordinates of point **P** with respect to the centre of the ellipse, **C**, are

$(\omega' - \omega_c)$ and $(p' - p_c)$, respectively. We can then infer that ω_c and p_c in Equations (28) and (29) are *negative* numbers. The immediate implication is that the signs of a and e, as well as the signs of c and d, must be opposite in Equation (21), as concluded from Equation (29). Note, however, that a and c should be positive, given that they are proportional to the coefficients k_ω and k_s, which, in turn, are functions of the pump/motor geometry (see Equations (5), (16) and (27)). Consequently, e and d should be negative. This implies in $T_0 < 0$ and $q_0 < 0$ for models where $\phi_3 = 1$ (Equation (27)), and whose efficiency level-curves are elliptical. In this case, the interpretation of q_0 and T_0 as being flow and torque losses, suggested by Wilson (1949) makes no sense (see comments on q_r and T_c after Equation (9)). On the other hand, if the level-curve is a first quadrant hyperbole as in Figure 2(a), $c < 0$ and $d > 0$ in Equation (28), which implies in $T_0 > 0$ and $q_0 < 0$. In this case, T_0 can be seen as torque loss. Nevertheless, given the non-applicability of such reasoning to every efficiency value, we still suggest to view T_0 as a correction to errors induced by measurement uncertainties.

Choosing $\phi_3 = 0$ in Equation (27) would produce a model unable to represent the curves in Figure 2(a) since this choice would imply that $d = e = 0$ in Equation (21) and, consequently, $\omega_c = p_c = 0$ in Equation (27). As a result, the ellipse in Figure 4 would need to be centred at point $(p = 0, \omega = 0)$, which does not correspond to any curve in Figure 2(a).

4. Experimental data fitting

Figure 5 shows the overall efficiency curves obtained for a typical axial-piston pump (Sauer-Danfoss 2010). Some randomly selected points in the inner and outer curves are also shown in the figure. They will be used later for data fitting. The curves are drawn relatively to the normalised pressure and speed values, ω and p. Normalised data are defined by the ratio between the actual data and some pre-defined rated (maximum) value. The curves in Figure 5 have been obtained for

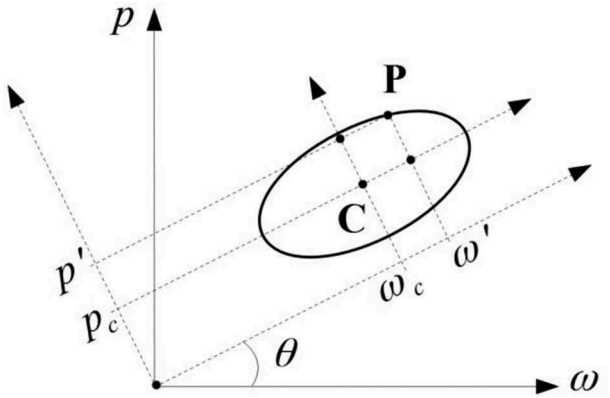

Figure 4. Rotation of coordinates for the ellipse.

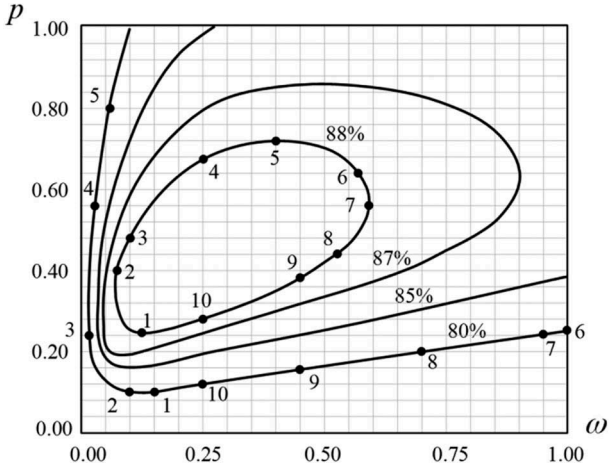

Figure 5. Typical efficiency curves for axial piston pumps (numbered dots have been randomly chosen for data fitting).

the maximum pump displacement. The procedures to be developed in this section equally apply to motors, as well to other pump models whose efficiency charts show a similar pattern.

From Figure 5 we see that the highest efficiency curve resembles an ellipse rotated relatively to the horizontal axis. The other curves appear to slowly 'open up' into hyperbolas as the overall efficiency is reduced. We believe that the fact that experimental plots, whenever provided by manufactures, show a similar pattern is no mere coincidence and indicates that the theoretical model given by Equations (21) and (27) is, in its very essence, correct.

Several methods have been proposed to fit a conic curve to a set of experimental points (see, for example, Fitzgibbon *et al.* 1996, Szpak *et al.* 2012, the references therein). In what follows, we describe the least-squares method that will be used in this paper. First, we note that Equation (21), can be written as

$$\mathbf{a}^{\mathrm{T}}\mathbf{D} = 0 \tag{30}$$

where:

$$\begin{cases} \mathbf{D}^{\mathrm{T}} = \begin{bmatrix} \omega^2 & \omega p & p^2 & \omega & p & 1 \end{bmatrix} \\ \mathbf{a}^{\mathrm{T}} = \begin{bmatrix} a & b & c & d & e & f \end{bmatrix} \end{cases} \tag{31}$$

Considering each of the N selected points on the experimental curves, $(\omega_i, p_i) \ldots (\omega_N, p_N)$, Equation (30) produces a point-wise error, R_i, given by the following relation

$$R_i = \mathbf{a}^{\mathrm{T}}\mathbf{D}_i = a\omega_i^2 + b\omega_i p_i + cp_i^2 + d\omega_i + ep_i + f \tag{32}$$

The least-squares approach seeks to minimise $R = \sum_{i=1}^{N} R_i^2$, which can be written as

$$R = \sum_{i=1}^{N} \left(\mathbf{a}^{\mathrm{T}}\mathbf{D}_i\right)^2 = \sum_{i=1}^{N} \mathbf{a}^{\mathrm{T}}\left[\mathbf{D}_i\left(\mathbf{D}_i^{\mathrm{T}}\mathbf{a}\right)\right] = \mathbf{a}^{\mathrm{T}}\mathbf{S}\mathbf{a} \tag{33}$$

where $\mathbf{S} = \sum_{i=1}^{N}\left(\mathbf{D}_i\mathbf{D}_i^{\mathrm{T}}\right)$

In order to minimise R, we follow Fitzgibbon *et al.* (1996) and use a Lagrange multiplier procedure (Halir and Flusser 1998). For example, consider the experimental points $(\omega_i, p_i) \ldots (\omega_N, p_N)$ on the curve $\eta = 88\%$ in Figure 5. We infer that the best-fit curve is an ellipse and place the constraint that $b^2 - 4ac > 0$ to Equation (33). Such constraint can be written in matrix form as $\mathbf{a}^T\mathbf{C}\mathbf{a} > 0$, where $\mathbf{C}$ is a 6×6 matrix filled with zeros except for the elements $C_{13} = C_{31} = 2$ and $C_{22} = -1$.

The inequality $\mathbf{a}^T\mathbf{C}\mathbf{a} > 0$ can be written as an equation if we define $\phi > 0$ such that $\mathbf{a}^T\mathbf{C}\mathbf{a} = \phi$. We, thus, seek to minimise $\mathbf{a}^T\mathbf{S}\mathbf{a}$ subject to the condition $\mathbf{a}^T\mathbf{C}\mathbf{a} - \phi = 0$. The problem is then formulated in terms of the Lagrange multiplier, λ, as

$$\nabla\left(\mathbf{a}^T\mathbf{S}\mathbf{a}\right) = \lambda\nabla\left(\mathbf{a}^T\mathbf{C}\mathbf{a} - \phi\right) \tag{34}$$

Equation (34) can be developed as follows:

$$\begin{bmatrix} \frac{\partial\left(\mathbf{a}^T\mathbf{S}\mathbf{a}\right)}{\partial A} \\ \vdots \\ \frac{\partial\left(\mathbf{a}^T\mathbf{S}\mathbf{a}\right)}{\partial F} \end{bmatrix} = \lambda \begin{bmatrix} \frac{\partial\left(\mathbf{a}^T\mathbf{C}\mathbf{a}\right)}{\partial A} \\ \vdots \\ \frac{\partial\left(\mathbf{a}^T\mathbf{C}\mathbf{a}\right)}{\partial F} \end{bmatrix} \tag{35}$$

It can be shown that Equation (35) simplifies to

$$\mathbf{S}\mathbf{a} = \lambda\mathbf{C}\mathbf{a} \tag{36}$$

Equation (36) can be combined with the constraint $\mathbf{a}^T\mathbf{C}\mathbf{a} = \phi$, resulting in $\mathbf{a}^T\mathbf{S}\mathbf{a} = \lambda\phi$. Since ϕ is arbitrary, the smallest possible absolute value for the Lagrange multiplier, λ, will also minimise $R = \mathbf{a}^T\mathbf{S}\mathbf{a}$, given by Equation (33). Note that the same could have been said if we were approximating a hyperbole, in which case, we would have $\phi < 0$. In any case, the smallest absolute value of λ would still minimise the error, R. Now, in order to find the minimum value of the constant λ, we rearrange Equation (36) and solve the following eigenvalue problem

$$\left(\frac{1}{\lambda}\right)\mathbf{a} = \left[\mathbf{S}^{-1}\mathbf{C}\right]\mathbf{a} \tag{37}$$

The eigenvector corresponding to the smallest absolute value of λ, contains the coefficients of the fitted ellipse we seek to obtain. As an example, consider the coordinates (ω_i, p_i) of the selected points in Figure 5, obtained after a visual inspection of the figure and given in Table 1.

After substitution of the values from Table 1 into $\mathbf{D}_i^T = \begin{bmatrix} \omega_i^2 & \omega_i p_i & p_i^2 & \omega_i & p_i & 1 \end{bmatrix}$ and then into $\mathbf{S} = \sum_{i=1}^{N}\left(\mathbf{D}_i\mathbf{D}_i^T\right)$, the smallest absolute values of λ and their corresponding eigenvectors in Equation (37) can be calculated. Finally, the rotated conic equation that minimises the error is obtained. Table 2 shows the results.

Figure 6 compares the two extreme curves shown in Figure 5 to the curves obtained through the equations given in Table 2. We observe that the two limiting cases, corresponding to $\eta_p = 80\%$ and $\eta_p = 88\%$, are easy to fit. The curves for $\eta_p = 85\%$, and $\eta_p = 87\%$, on the other hand, are difficult to be characterised as conic curves. However, at this point, we might ask the question of whether it is possible to interpolate the curves and obtain a model that can predict the pump's behaviour over the whole range of efficiency values and still remain accurate, within an acceptable tolerance. We deal with this matter in the following section.

5. Extension to other efficiency values

We have mentioned that the curves for $\eta_p = 85\%$ and $\eta_p = 87\%$ are difficult to be fit by conics in Figure 6. Therefore, if we are seeking a model that approximates the efficiency level curves in a very precise manner, we need to resort to more complex polynomial curves, where terms in ω^k and p^k $(k \geq 0)$ are added to Equation (21). However, if a simpler model that is still able to compute efficiency values within an acceptable error margin is desired, we may want to consider interpolating the conic curves between extreme values.

Table 1. Coordinate values for the nodes shown in Figure 5.

η_p	Point	1	2	3	4	5	6	7	8	9	10
80%	ω_i	0.015	0.100	0.025	0.030	0.060	1.000	0.950	0.700	0.450	0.250
	p_i	0.100	0.100	0.240	0.560	0.800	0.260	0.240	0.200	0.160	0.120
88%	ω_i	0.125	0.070	0.100	0.250	0.400	0.560	0.590	0.550	0.450	0.250
	p_i	0.241	0.400	0.480	0.660	0.720	0.640	0.560	0.440	0.380	0.280

Table 2. Best fit curve equations.

$\eta_p = 80\%$	Minimum eigenvalue	$\lvert\lambda\rvert_{\min} = \left\lvert -\frac{1}{12782}\right\rvert$
	Corresponding eigenvector	$\mathbf{a}^T = [\ -0.176 \quad 0.976 \quad -0.010 \quad -0.071 \quad 0.033 \quad -0.004\ ]$
	Conic equation	$0.176\omega^2 - 0.976\omega p + 0.010p^2 + 0.071\omega - 0.033p + 0.004 = 0$
$\eta_p = 88\%$	Minimum eigenvalue	$\lvert\lambda\rvert_{\min} = \left\lvert\frac{1}{7458}\right\rvert$
	Corresponding eigenvector	$\mathbf{a}^T = [-0.467 \quad 0.499 \quad -0.591 \quad 0.062 \quad 0.415 \quad -0.086\ ]$
	Conic equation	$0.467\omega^2 - 0.499\omega p + 0.591p^2 - 0.062\omega - 0.415p + 0.086 = 0$

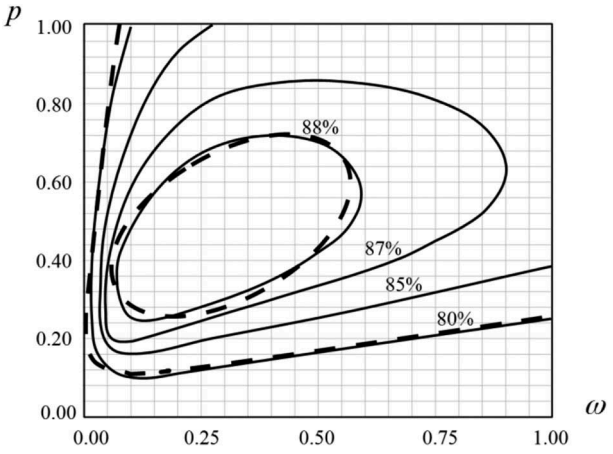

Figure 6. Comparison between best fitting curves (dashed lines) and experimental data (solid lines).

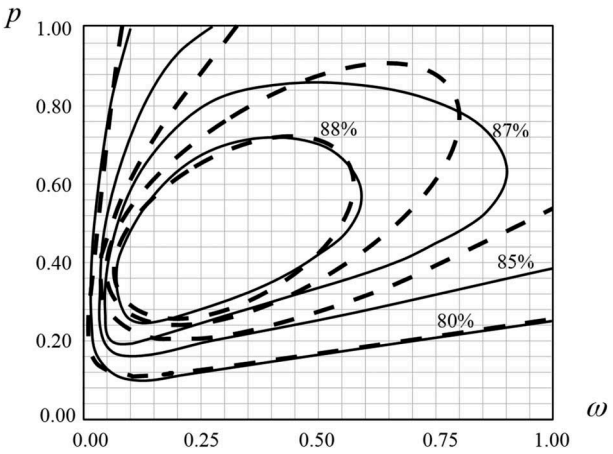

Figure 7. Comparison between best fit curves (dashed lines) and experimental data (solid lines).

If we assume a linear interpolation for the coefficients a through f in Equation (21) between the two efficiency values, $\eta_0 = 80\%$ and $\eta_1 = 88\%$

$$\begin{cases} a = \left[a_0 - \left(\frac{a_1 - a_0}{\eta_1 - \eta_0}\right)\eta_0\right] + \left(\frac{a_1 - a_0}{\eta_1 - \eta_0}\right)\eta_p = A_0 + k_a\eta_p \\ \vdots \\ f = \left[f_0 - \left(\frac{f_1 - f_0}{\eta_1 - \eta_0}\right)\eta_0\right] + \left(\frac{f_1 - f_0}{\eta_1 - \eta_0}\right)\eta = F_0 + k_f\eta_p \end{cases} \tag{38}$$

If we substitute the coefficients $a \ldots f$, obtained from Equation (38) into Equation (21), we obtain

$$\eta_p = -\frac{A_0\omega^2 + B_0\omega p + C_0 p^2 + D_0\omega + E_0 p + F_0}{k_a\omega^2 + k_b\omega p + k_c p^2 + k_d\omega + k_e p + k_f} \tag{39}$$

Figure 7 compares the curves for $\eta = 80\% \ldots 88\%$ in Equation (39), with the catalogue data. The curves do not coincide for all values of ω and p but note the error is always smaller than 2%.

Equation (39) can be used to plot the efficiency as a function of pressure and flow (relative values). The three-dimensional efficiency surface, as well as some representative constant pressure curves are shown in Figure 8.

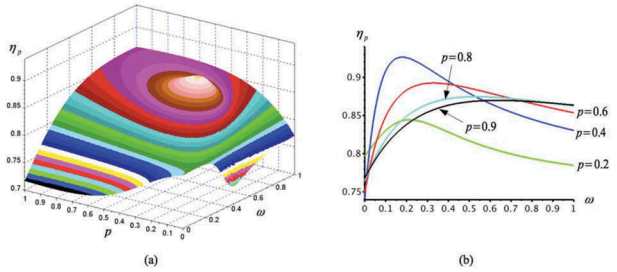

Figure 8. Three-dimensional efficiency surface and (b) constant pressure curves.

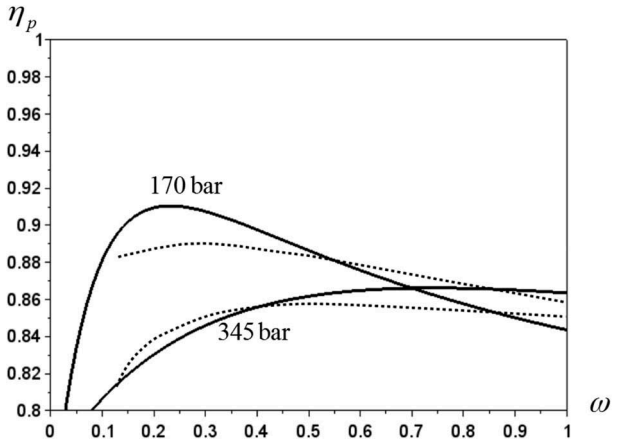

Figure 9. Efficiency curves for selected pressure values.

Figure 9 shows a cross-cut of Figure 8 for $p = 0.493$ and $p = 1$. For a rated pressure of 345bar, these two relative pressure values correspond to 170 and 345bar, respectively. Dashed lines represent catalogue data (Sauer-Danfoss 2010). Again, the difference between model and catalogue values remains smaller than 2% for the whole speed range.

6. Conclusions

In this paper, we showed that three-dimensional overall efficiency surfaces are naturally obtained if we start from the correct efficiency definition, which differs from the usual 'volumetric times mechanical efficiency' formula. By using a slightly modified version of the overall efficiency expression, we arrived at a general rotated conic equation, which correctly reproduces the trends found in usual efficiency diagrams provided by pump and motor manufacturers. In fact, using the practical example of a commercial pump, we obtained a set of level curves for the overall efficiencies that differed by less than 2% from the actual experimental data. No more than simple linear equations based on classic volumetric and mechanical loss models were needed in the process.

7. Nomenclature

p:	pressure differential between pump and motor ports
ω:	angular speed of the pump/motor shaft
u:	fluid velocity
μ:	absolute viscosity
R, B, L, C:	pump/motor geometric dimensions (Figure 1)
D:	pump/motor displacement
D_m:	maximum pump/motor displacement
x:	displacement ratio ($x = D/D_m$)
q_p, q_m:	pump/motor flow
T_p, T_m:	pump/motor torque
q_L:	flow losses
q_β:	compressibility flowrate
β:	bulk modulus
T_L:	torque losses
$K_u, K_s, k_s,$ $K_\omega, k_\omega, C_s C_\omega,$ $C_p, \phi_1, \phi_2, \phi_3$:	loss coefficients
q_r, T_c:	cavitation and 'pressure independent friction' losses
q_0, T_0:	flow and torque correction terms
η_p^v, η_p^m:	volumetric and mechanical efficiencies of the pump
η_m^v, η_m^m:	volumetric and mechanical efficiencies of the motor
η_p, η_m:	overall efficiencies of the pump and motor
a_p, $b_p \cdots$ f_m, f_m:	level curves coefficients for the pump and the motor
P_i, P_o:	power input and output at the pump/motor
H_0:	pump/motor constant losses
q_{pi}, q_{po}:	pump input and output flows
q_{mi}, q_{mo}:	motor input and output flows

Disclosure statement

No potential conflict of interest was reported by the authors.

Funding

This work was supported by the Natural Sciences and Engineering Research Council of Canada [RGPIN 121353–2013].

Notes on contributors

Gustavo Koury Costa works at the Federal Institute of Education, Science and Technology in Recife-PE, Brazil. He received his MSc and DSc degrees from the Federal University of Pernambuco, Brazil. He did his Post-Doctorate in the University of Manitoba, Canada, having become adjunct professor for the Faculty of Mechanical Engineering.

Nariman Sepehri is a professor with the Department of Mechanical Engineering, at the University of Manitoba, Canada. He received MSc and PhD degrees from the University of British Columbia, Canada. His research and development activities are primarily centred in all fluid power-related aspects of systems, manipulation, diagnosis, and control.

References

Akers, A., Gassman, M., and Smith, R., 2006. *Hydraulic power system analysis*. USA: CRC Press.

Blackburn, J.F., Reethof, G., and Shearer, J.L., 1960. *Fluid power control*. USA: Technology press of M.I.T. and John Wiley & Sons.

Costa, G.K. and Sepehri, N., 2015. *Hydrostatic transmissions and actuators – operation, modelling and applications*. UK: John Wiley & Sons.

Doddannavar, A. and Barnard, A., 2005. *Practical hydraulic systems: operation and troubleshooting for engineers and technicians*. Elsevier, US.

Dorey, R.E., 1988. Modelling of losses in pumps and motors. *First Bath International fluid power workshop*, September. UK: University of Bath, 71–97.

Esposito, A., 1980. *Fluid power with applications*. 4th ed. USA: Prentice Hall.

Fitzgibbon, A.W., Pilu, M., and Fisher, R.B., 1996. Direct least squares fitting of ellipses. *IEEE transactions on pattern analysis and machine intelligence*, 21 (5), 476–480. doi:10.1109/34.765658

Halir, R. and Flusser, J., 1998. Numerically stable direct least squares fitting of ellipses. *Proceedings of the 6th International conference in Central Europe on computer graphics and visualization*, Pizen, Czech Republic: WSCG, pp 125–132.

Hall, S.J. and Steward, B.L., 2014. Comparison of steady state flow loss models for axial piston pumps. *In: International Fluid Power Exposition (IFPE), Paper 4.1*, Las Vegas, US.

Ivantysyn, J. and Ivantysynova, M., 2000. *Hydrostatic pumps and motors, principals, designs, performance, modeling, analysis, control and testing*. New Delhi: Academia Books International.

Jeong, H., 2007. A novel performance model given by the physical dimensions of hydraulic axial piston motors: model derivation. *Journal of Mechanical Science and Technology*, 21 (1), 83–97. doi:10.1007/BF03161714

Jung, D.S., Kim, H.E., Jeong, H.S., Kang, B.S, Lee, Y.B., Kim, J. K., Kang, E.S., 2005. Experimental study on the performance estimation efficiency model of a hydraulic axial piston motors. *Proceedings of the 6th JFPS International symposium on fluid power*, TSUKUBB, 284–290. 2A3–1, Japan Fluid Power System Society - JFPS.

Kluger, M.A., Fussner, D.R., and Roethler, B., 1996. A performance comparison of various automatic transmission pumping systems. *SAE International congress & exposition*, Detroit, US, 33–40. doi:10.1016/S0940-2993(96)80089-3

KohmäScher, T., *et al.*, 2007. Improved loss modeling of hydrostatic units: requirement for precise simulation of mobile working machine drivelines. *In: ASME 2007 International mechanical engineering congress and exposition volume 4: design, analysis, control and diagnosis of fluid power systems*, ASME, Seattle, WA.

Manring, N.D., 2005a. *Hydraulic control systems*. US: John Wiley & Sons.

Manring, N.D., 2005b. Measuring pump efficiency: uncertainty considerations. *Journal Energy Resources Technological*, 127 (4), 280–284. doi:10.1115/1.1926311

Manring, N.D., 2016. Mapping the efficiency for a hydrostatic transmission. *Journal of Dynamic Systems, Measurement, and Control*, 138, 0310041–0310048. doi:10.1115/1.4032289

McCandlish, D. and Dorey, R.E., 1984. The mathematical modeling of hydrostatic pumps and motors. *Proceedings of the Institution of Mechanical Engineers*, 198B (10), 165–174. doi:10.1243/PIME_PROC_1984_198_062_02

Merritt, H.E., 1967. *Hydraulic control systems*. US: John Wiley & Sons.

Sauer-Danfoss, 2010. *Series 40 axial piston pumps technical information*. US. October. 520L0635 Rev EJ - Sauer-Danfoss, US.

Stringer, J., 1976. *Hydraulic system analysis: an introduction*. US: John Wiley & Sons.

Szpak, Z.L., Chojnacki, W., and Van Den Hengel, A., 2012. Guaranteed ellipse fitting with the Sampson distance. *Proceedings of the 12th European conference on computer vision, Part V*, 7–13 October. Florence, Italy.

Tessmann, R.K., 1979. A leakage path model for a hydraulic pump. *The B.F.P.R Journal*, 12 (1), 5–9.

Watton, J., 2009. *Fundamentals of fluid power control*. Cambridge University Press, UK.

Wilson, W.E., 1946. Rotary-pump theory. *ASME Transactions*, 68, 371–384.

Wilson, W.E., 1949. Performance criteria for positive-displacement pumps and fluid motors. *ASME Transactions*, 71 (2), 115–120.

Zarotti, G.L. and Nervegna, N., 1981. Pump efficiencies approximation and modelling. *6th International fluid power symposium, Paper C4*, Cambridge, UK. 145–164.